Citation: Clin. Transl. Sci. (2019) 12, 400–407; doi:10.1111/cts.12630

ARTICLE

Interaction Between Sex and Organic Anion-Transporting Polypeptide 1b2 on the Pharmacokinetics of Regorafenib and Its Metabolites Regorafenib-N-Oxide and Regorafenib-Glucuronide in Mice

Qiang Fu[1], Mingqing Chen[1], Jason T. Anderson[1], Xinxin Sun[1], Shuiying Hu[1], Alex Sparreboom[1] and Sharyn D. Baker[1,*]

Regorafenib, a multikinase inhibitor used in the treatment of various solid tumors, undergoes extensive uridine 5′-diphosphate glucuronosyltransferase (Ugt)1a9-mediated glucuronidation to form regorafenib-N-β-glucuronide (M7; RG), but the contribution of hepatic uptake transporters, such as organic anion-transporting polypeptide (Oatp)1b2, to the pharmacokinetics of regorafenib remains poorly understood. Using NONMEM-based, population-based, parent-metabolite modeling, we found that Oatp1b2 and sex strongly impact the systemic exposure to RG in mice receiving oral regorafenib. Metabolic studies revealed that the liver microsomal expression of cytochrome P450 (Cyp)3a11 is twofold lower in female mice, whereas Ugt1a9 levels and function are not sex dependent. This finding is consistent with the metabolism of regorafenib occurring via two competing pathways, and the lack of Oatp1b2 results in decreased clearance of RG. The described model provides mechanistic insights into the *in vivo* disposition of regorafenib.

Study Highlights

WHAT IS THE CURRENT KNOWLEDGE ON THE TOPIC?
☑ The multikinase inhibitor regorafenib undergoes extensive uridine 5′-diphosphate glucuronosyltransferase (Ugt)1a9-mediated formation to regorafenib-β-D-glucuronide (RG). Xenobiotic glucuronides can be taken up from the circulation into hepatocytes by organic anion-transporting polypeptide (Oatp)1b2 and subsequently undergo biliary secretion.

WHAT QUESTION DID THIS STUDY ADDRESS?
☑ Here, we experimentally addressed the question to what extent the transport of RG is affected by Oatp1b2 deficiency in mice.

WHAT DOES THIS STUDY ADD TO OUR KNOWLEDGE?
☑ Our findings suggest the possibility that impaired Oatp1b2 function can lead to altered pharmacokinetic properties of regorafenib metabolites in a sex-dependent manner, in particular when cytochrome P450 (Cyp)3a11 activity is impaired.

HOW MIGHT THIS CHANGE CLINICAL PHARMACOLOGY OR TRANSLATIONAL SCIENCE?
☑ The current observations with regorafenib may have relevance to other xenobiotics undergoing phase II conjugation through glucuronidation.

Regorafenib is an oral multikinase inhibitor approved for the treatment of metastatic colorectal cancers,[1] gastrointestinal stromal tumors,[2] and hepatocellular carcinomas.[3] Compared with conventional cytotoxic chemotherapeutics, regorafenib has demonstrated activity against a variety of diseases that were previously essentially resistant to standard chemotherapy and reduced toxicity to normal tissues. However, the agent is still afflicted by some of the same problems observed with cytotoxic chemotherapeutics, such as extensive interindividual pharmacokinetic variability and the existence of a poorly defined therapeutic window.[4] In addition, the clinical use of regorafenib has been associated with the occurrence of debilitating toxicities, including hand-foot skin reactions, diarrhea, and hypertension reactions.[5]

Similar to the related multikinase inhibitor sorafenib,[6] the elimination pathways of regorafenib involve both hepatic metabolism to the metabolite regorafenib-N-oxide (M2)[7] and conjugation to the metabolite regorafenib-N-β-glucuronide (M7; RG).[8] It has been suggested that both regorafenib and sorafenib can undergo enterohepatic recirculation, a process that involves removal of solutes from blood by uptake into hepatocytes, secretion into bile, and intestinal reabsorption, sometimes accompanied by hepatic conjugation and intestinal deconjugation of glucuronide metabolites.[6,9] Although the occurrence of enterohepatic recirculation of regorafenib has not been experimentally verified, it provides plausible explanation for the prolonged half-life of regorafenib levels in plasma observed in patients with cancer.[4]

[1]Division of Pharmaceutics and Pharmaceutical Chemistry and Comprehensive Cancer Center, College of Pharmacy, The Ohio State University, Columbus, Ohio, USA.
*Correspondence: Sharyn D. Baker (baker.2480@osu.edu)
Received: September 25, 2018; accepted: February 2, 2019. doi:10.1111/cts.12630

We recently reported that mice lacking the organic anion-transporting polypeptide (Oatp)1b2 (Oatp1b2 (–/–) mice)), an uptake transporter localized to the sinusoidal (basolateral) membrane of hepatocytes, experience substantially increased plasma levels of sorafenib-glucuronide after oral sorafenib administration.[10] Based on the broad substrate specificity of Oatp1b2,[10,11] it is possible that other xenobiotic glucuronides, including RG, are subject to the same hepatocellular disposition process. The aims of this study were to evaluate the role of Oatp1b2 in the pharmacokinetics of regorafenib and its metabolites regorafenib-N-oxide (M2)[7] and RG (M7)[7] and to determine covariates that are primary drivers of the variability in population pharmacokinetic parameters of these agents.

METHODS

Chemicals and reagents

Regorafenib was purchased from LC Laboratories (> 99% purity; Woburn, MA), RG was purchased from Toronto Research Chemicals (> 99% purity; North York, ON, Canada), and regorafenib-N-oxide, regorafenib-[13]-CD3, and regorafenib-N-oxide-[13]-CD3 were obtained from Clearsynth (> 99% purity; Mississauga, ON, Canada). Sorafenib was obtained from Chemie Tek (> 99% purity; Indianapolis, IN), and sorafenib-N-oxide and sorafenib-glucuronide were obtained from Toronto Research Chemicals (> 99% purity). [2H3,15N]-sorafenib was obtained from Alsachimie (> 99% purity; Strasbourg, France), and sorafenib-glucuronide-[13] CD3 was produced as described previously.[10] Mouse liver microsomes were obtained from 10 DBA/1lacJ strain wild-type mice. The human uridine 5′-diphosphate glucuronosyltransferase (Ugt) supersome metabolic enzymes were obtained from Corning (Wobum, MA), and methanol, and acetonitrile, and water (liquid chromatography and mass spectroscopy grade) from Fisher Scientific (Fair Lawn, NJ).

Animals and study design

All experiments were performed in Oatp1b2 (–/–) mice or wild-type mice on a DBA/1lacJ background strain according to a protocol approved by the Ohio State University Laboratory Animal Resources and Animal Care and Use Committee. The dosing solution of regorafenib was prepared at a final concentration of 2 mg/mL in a mixture of Cremophor EL:transcutol:0.9% sodium chloride (1:1:5, vol/vol/vol), and administered orally at a dose of 10 mg/kg. Blood samples of 30 μL were obtained from individual mice at 0.25, 0.5, 1.5, 3, 4.5, and 7.5 hours after administration. Samples at the 0.25–1.5 hour timepoints were taken from the submandibular vein, samples at 3 and 4.5 hours were obtained from the posterior iliac venous plexus, and a final sample was obtained at 7.5 hours by cardiac puncture. Blood samples were processed by centrifugation (3,000*g*, 4°C) in heparin-containing tubes, and plasma supernatants were stored in 0.5-mL tubes at –80°C until analysis. For comparative purposes, additional pharmacokinetic studies were performed in the same mouse models following the administration of sorafenib, according to procedures described by us previously.[10]

Metabolite profiling

Regorafenib (10 μM) was incubated at 37°C with nicotinamide adenine dinucleotide phosphate–fortified mouse liver microsomes (1 mg/mL) or Ugt supersomes of Ugt1a1, Ugt1a3, Ugt1a4, Ugt1a6, Ugt1a7, Ugt1a8, Ugt1a9, Ugt1a10, Ugt2b4, Ugt2b7, or Ugt2b15 (0.5 mg/mL) in potassium phosphate buffer (100 mM, pH 7.4; total volume, 200 μL). The number of replicate observations was $n = 4$ for mouse liver microsomes and $n = 3$ for Ugt supersomes. Protein concentrations were determined using the Pierce BCA Protein Assay. Reactions were terminated at 60 minutes with acetonitrile, and supernatant fractions were analyzed by ultra-performance liquid chromatography–tandem mass spectrometry, as previously described.[8]

Real-time reverse transcriptase polymerase chain reaction analyses

RNA was isolated from various mouse tissues (30 mg), homogenized, and then extracted using EZNA Total RNA Kit extraction kit (Omega Bio-tek, Norcross, GA). The complementary DNA was generated from 2 μg of RNA using qScript XLT cDNA Supermix (Quantabio, Beverly, MA). Real-time reverse transcriptase polymerase chain reaction was performed with TaqMan probes (Thermo Fisher Scientific, Waltham, MA) and TaqMan Fast reagents. Reactions were carried out in triplicate and normalized to glyceraldehyde 3-phosphate dehydrogenase.

Analytical method

The analytical method of sorafenib and its metabolites was described in a previous study.[10] Concentrations of regorafenib and its metabolites in plasma samples were determined by a validated method based on ultra-performance liquid chromatography–tandem mass spectrometry using analytical and extraction conditions described in detail elsewhere.[8] The analytical system was comprised of a Vanquish UHPLC system and a TSQ Quantiva mass spectrometer (Thermo Fisher Scientific). Results from assay validation studies revealed that the within-day precision, between-day precision, and accuracy were < 8.42%, < 8.10%, and < 7.42%, respectively. The lower limit of quantification was 5 ng/mL.

Pharmacokinetic analysis

Noncompartmental pharmacokinetic analysis was evaluated by the WinNonlin software version 7.6 (Certara, Princeton, NJ). The area under the concentration–time curve (AUC) is calculated according to the linear trapezoidal rule until the last timepoint (AUC_{last}), the measurable target analyte concentration. The peak plasma concentration (C_{max}) and the time to peak plasma concentration (T_{max}) were obtained by visual inspection of data from the concentration–time curve. The elimination rate constant was estimated from the slope of the end of the log plasma concentration–time curve fitted by the least squares method, and the terminal half-life ($t_{1/2}$) was calculated to be 0.693/elimination rate constant. Statistical significance in pharmacokinetic parameters between groups was determined with an unpaired two-sided paired *t*-test.

Nonlinear mixed-effect model development was performed using NONMEM software version 7.3 and PDx-Pop 5.0 (ICON Development Solutions, Ellicott City, MD). Postprocessing of graphical plots in NONMEM was performed using S-PLUS version 8.0 (Insightful, Seattle, WA) and Rstudio version 1.14 (Rstudio, Boston, MA). The population pharmacokinetics of regorafenib and its metabolites were analyzed in a stepwise manner. Similar methods involving transporter-mediated pharmacokinetic profiles have been applied to levofloxacin and glycylsarcosine.[12,13] All models were created using the first-order conditional estimation method, and the subroutine ADVAN6 was used to describe all model kinetics process, which included interindividual and residual variabilities. The model determination was guided by the minimum objective function value, Akaike Information Criterion, and visual inspection of diagnostic plots.

Base model development

In the initial development of the base model, the best structural model for regorafenib involved first order absorption in a two-compartment pharmacokinetic model. Subsequently, regorafenib-N-oxide data were fitted to a one-compartment model with first order disposition to connect to the central compartment of regorafenib. Regorafenib-glucuronide undergoing enterohepatic circulation was modeled with a semiphysiological model in which a fraction of RG from the metabolite compartment is excreted from hepatocytes into the gallbladder with a first order rate into the last gastrointestinal transit compartment.[14] Next, RG was assumed to undergo partial conversion back to regorafenib followed by its reabsorption into the central compartment. Once the best metabolite structural population pharmacokinetic model was developed, all pharmacokinetic parameters were estimated at the same time using the ADVAN 6 routine in NONMEM. Values representing the metabolism of regorafenib-N-oxide (F_{MET1}), the metabolism of RG (F_{MET2}), the excretion of RG from the central compartment to the gall bladder (F_{EHC}), and the deconjugation of RG to regorafenib (T_{EHC}) were fixed based on published human data.[9]

Interindividual variability (IIV) of the parameters was used to account for the population pharmacokinetics model in Eq. 1. The value of the parameter for the individual is P_i, whereas the value of the parameter for the population is P_{pop}. The η in the IIV represents random effects by mean of zero and variance ω^2. The coefficient of variation (%CV) was used to represent the magnitude of IIV. Residual variability was sculptured by a log-error model, as described in Eq. 2. C_{ij} and $C_{pred,ij}$ indicate the jth determinate with prediction of regorafenib, regorafenib-N-oxide, and RG concentrations in the model. The individual ε_{ij} refer to the additional residual random error for individual i and observation j. The ε random effects were assumed to be distributed in a balanced manner with a mean of zero and variance σ^2.

$$P_i = P_{pop} \cdot \exp(\eta_i) \quad (1)$$

$$\ln C_{ij} = \ln C_{pred,ij} + \varepsilon_{ij} \quad (2)$$

Covariate analysis was performed to identify an additive chance variable that can explain the variability observed in the parameter estimates. Covariates were initially analyzed by visual inspection. Significance was tested by the stepwise elimination, and a minimum objective function value change of 3.84 and 10.83 were used as significance cutoffs at the level of 0.5% and 0.1% in backward elimination models. The significance of sex and Oatp1b2 as two covariates was evaluated as described in Eqs. 3 and 4, where θ_1 and θ_3 as a parameter without an impact of sex and Oatp1b2, and θ_2 and θ_4 represents a change in the parameter with an impact of sex and Oatp1b2.

$$P = \theta_1 \cdot (1 + \theta_2 \cdot \text{SEX}) \quad (3)$$

$$P = \theta_3 \cdot (1 + \theta_4 \cdot \text{Oatp1b2}) \quad (4)$$

Model evaluation

The validity of the population pharmacokinetics model was determined by goodness-of-fit analyses, which included observed concentrations (dependent variable, DV) vs. population predictions (PRED) and individual predictions, as well as conditional weighted residuals vs. PRED and time. Bootstrapping was used to evaluate the precision of the pharmacokinetic parameters and model strength, and 1,000 bootstrap runs were created with restated random sampling and backup from the NONMEM data sets. Bootstrap parameters, 95% confidence intervals, and SEs were compared with the original data set for parameter estimates, and model stability was evaluated in the final model.

RESULTS

Regorafenib pharmacokinetics in Oatp1b2 (–/–) mice

In order to verify whether regorafenib is a substrate for the Oatp1b2 type carrier *in vivo*, we determined regorafenib pharmacokinetic data from the pooled data obtained in male and female mice deficient for Oatp1b2 (Oatp1b2 (–/–) mice). Consistent with our previous pharmacokinetic study of sorafenib in mice,[10] we found that the observed C_{max} and AUC_{last} of regorafenib and regorafenib-N-oxide were minimally affected after a single oral dose of regorafenib by Oatp1b2 deficiency (**Figure 1**; **Table 1**). In contrast, we found that measures of systemic exposure to RG were significantly increased in Oatp1b2 (–/–) mice, resulting in 8.7-fold and 3.7-fold increases in exposure compared with female and male wild-type mice (**Figure 1c**; **Table 1**). Furthermore, compared with male mice the AUC_{last} and C_{max} of RG were higher in female mice compared with male mice, regardless of Oatp1b2 genotype status (**Table 1**).

Phenotypic characterization of Oatp1b2 (–/–) mice

Subsequent mechanistic studies were performed using mouse liver microsomes, and these confirmed that the formation of RG is mainly mediated by Ugt1a9 (**Figure 2a**), and that the rate of regorafenib glucuronidation is not significantly different between liver genotypes (**Figure 2b**). This suggests that the observed changes in levels of RG in Oatp1b2 (–/–) mice cannot be explained by an intrinsically

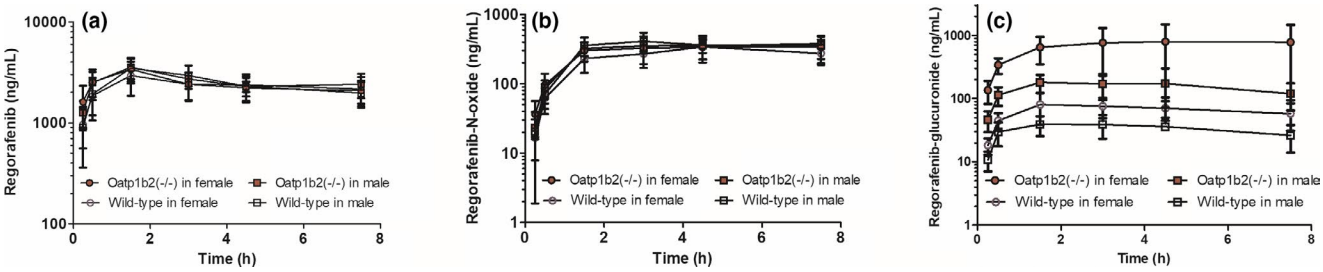

Figure 1 Influence of organic anion-transporting polypeptide (Oatp)1b2 deficiency and sex on regorafenib and its metabolites. Wild-type and Oatp1b2-deficient (Oatp1b2 (–/–)) male and female mice (N = 10/group) were given 10 mg/kg regorafenib via oral gavage. Plasma concentrations of (**a**) regorafenib, (**b**) regorafenib-N-oxide, and (**c**) regorafenib-glucuronide were determined by ultra-performance liquid chromatography–tandem mass spectrometry. Data represent the mean ± SD of 10 samples per timepoint.

Table 1 Noncompartmental pharmacokinetic analysis of regorafenib given as a single oral dose (10 mg/kg) in wild-type mice and Oatp1b2 (–/–) mice

	Regorafinib		Regorafenib-glucuronide		Regorafenib-N-Oxide	
	Female	**Male**	**Female**	**Male**	**Female**	**Male**
Wild-type mice						
C_{max} (ng/mL)	3,260 ± 762	3,500 ± 904	91.2 ± 36.0	58.4 ± 38.9	257 ± 105	451 ± 133
T_{max} (hour)	3.20 ± 2.20	1.65 ± 0.474	4.25 ± 1.84	4.30 ± 2.46	2.95 ± 1.76	2.70 ± 2.19
$t_{1/2}$ (hour)	14.0 ± 0.940	8.51 ± 2.79	–	–	–	–
AUC_{last} (μg × hour/mL)	17.3 ± 4.08	18.5 ± 4.78	0.466 ± 0.169*	0.278 ± 0.157	1.91 ± 0.453	2.49 ± 0.759
Oatp1b2(–/–) mice						
C_{max} (ng/mL)	3,670 ± 276	3,630 ± 779	806 ± 605†,*	217 ± 119†	344 ± 170	398 ± 58.6
T_{max} (hour)	1.39 ± 0.333	2.10 ± 1.90	4.67 ± 2.62	4.60 ± 2.37	2.85 ± 2.15	2.75 ± 1.60
$t_{1/2}$ (hour)	12.0 ± 5.35	11.5 ± 4.79	–	–	–	–
AUC_{last} (μg × hour/mL)	15.6 ± 7.14	19.3 ± 2.80	4.08 ± 3.84†,*	1.03 ± 0.427†	2.10 ± 0.972	2.29 ± 0.476

Data represent mean ± SD.
AUC_{last}, area under the plasma concentration–time curve; C_{max}, peak plasma concentration; Oatp, organic anion-transporting polypeptide; $t_{1/2}$, half-life of the terminal phase; T_{max}, time to peak plasma concentration.
An unpaired t-test *$P < 0.05$ female vs. male, †$P < 0.05$ Oatp1b2 (–/–) vs. wild-type mice (n = 10 per group).

altered regorafenib metabolic capacity. Interestingly, in samples from Oatp1b2 (–/–) mice, the rate of formation of regorafenib-N-oxide in liver microsomes was reduced (**Figure 2c**) and found to be substantially impaired in samples from female mice regardless of genotype without changes in corresponding expression of the Ugt1a9, cytochrome P450 (Cyp)3a11, and Oatp1b2 genes (**Figure 2d–f**). The male-dominant regorafenib-N-oxide formation rate in mouse-liver microsomes led us to re-examine the pharmacokinetic properties of regorafenib stratified by sex, and this analysis suggested that impaired Cyp3a11 activity results in shunting of regorafenib elimination to increased levels of RG in female mice (**Table 1**). This is not unique to regorafenib, as similar sex-dependent profiles were observed in mice following the administration of sorafenib (**Table 2**).

Sex-dependent population pharmacokinetics of regorafenib

To further explore the male-female differences in RG levels, population pharmacokinetic models for regorafenib, regorafenib-N-oxide, and RG were developed (**Figure 3**). In this model, values for the secretion of transferred RG from the peripheral compartment to the gallbladder and the rate of its deconjugation back to regorafenib were fixed based on mass balance data reported previously,[9] where a similar metabolite profile of regorafenib and metabolites was observed in human and mouse liver microsomes following a 60-minute incubation period.[15] Because the regorafenib metabolites were not administered alone, the volumes of distribution were fixed to 1 mL,[14] and the estimated metabolic fractions were understood as the ratio of regorafenib converted to regorafenib-N-oxide and RG. Goodness-of-fit plots for regorafenib and the metabolites suggest that the model fits were acceptable (**Figure S1**), with relative SEs ranging from 6.3–26.6% and with 99% of the data converging successfully (**Figure S2**). In the final population pharmacokinetic model (**Figure S3**), all the parameter estimates were within the 95% intervals in bootstrap analysis. In this model, sex and Oatp1b2 were found to be significant covariates on the metabolic clearance of RG (**Table 3**), with minimum objective function value changes of 64.15 and 32.69, respectively, for sex and Oatp1b2 genotype in backward elimination models (using significance cutoffs at the level of 0.1%), suggesting

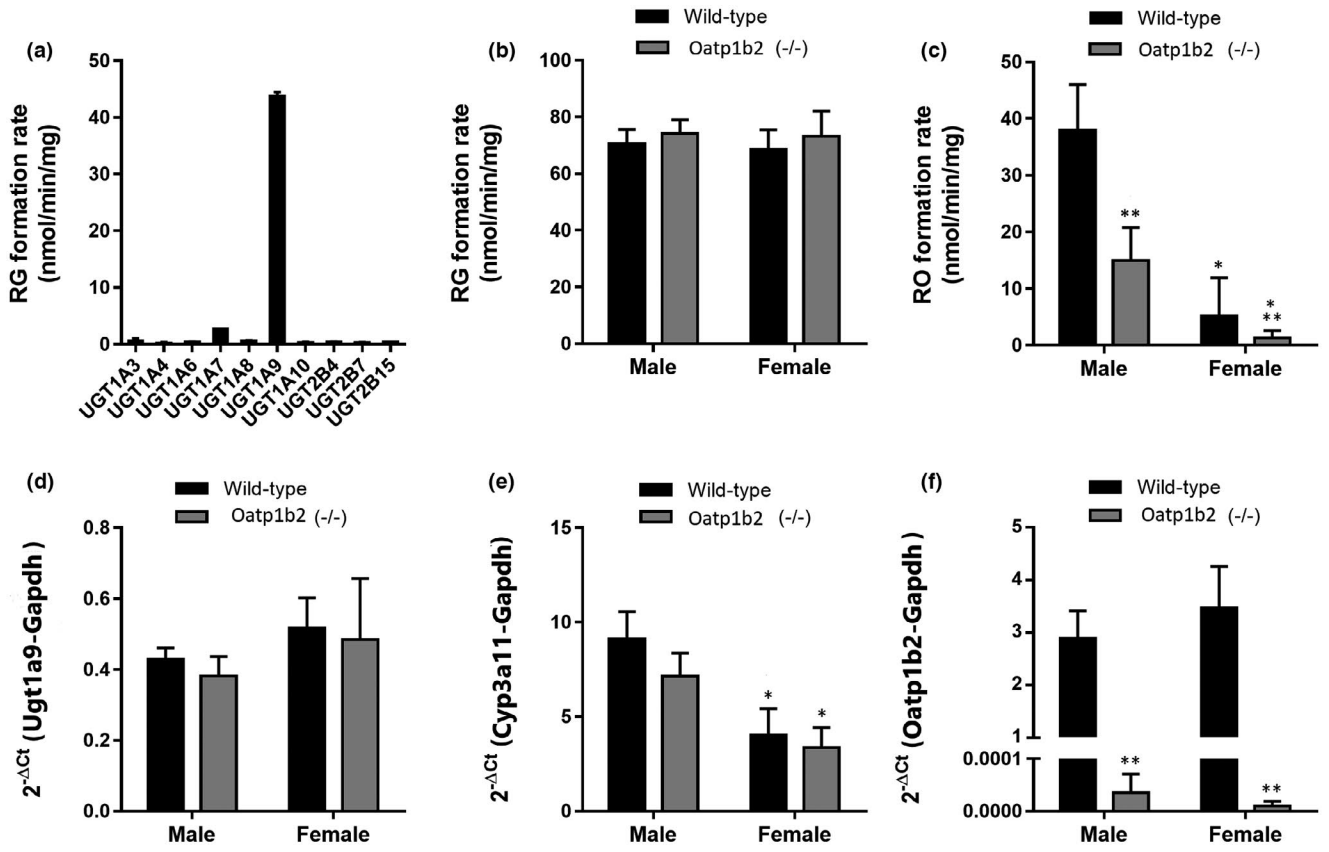

Figure 2 Metabolism of regorafenib. *In vitro* regorafenib-glucuronide (RG) formation was determined by (**a**) various recombinant human uridine 5′-diphosphate glucuronosyltransferase (Ugt) isozymes and (**b**) liver microsomes from male and female, wild-type and organic, anion-transporting polypeptide (Oatp)1b2(–/–) mice. (**c**) Similar experiments were performed for regorafenib-N-oxide. Data represent the mean ± SD of three (Ugt) or four (liver) samples. Real-time reverse transcriptase polymerase chain reaction was performed on mouse liver samples for (**d**) Ugt1a9, (**e**) Cyp3a11, and (**f**) Oatp1b2. Data represent the mean ± SD of 12 liver samples. **P* < 0.05 female vs. male mice; ***P* < 0.05 Oatp1b2 (–/–) vs. wild-type mice. Cyp, cytochrome P450; Gapdh, glyceraldehyde 3-phosphate dehydrogenase; RO, regorafenib-N-oxide.

Table 2 Noncompartmental pharmacokinetic analysis of sorafenib given as a single oral dose (10 mg/kg) in wild-type mice and Oatp1b2 (–/–) mice

	Sorafenib		Sorafenib-glucuronide		Sorafenib-N-oxide	
	Female	Male	Female	Male	Female	Male
Wild-type mice						
C_{max} (ng/mL)	5,850 ± 585	4,520 ± 937	249 ± 253	278 ± 146	136 ± 16.7	87.3 ± 30.5
AUC_{last} (μg × hour/mL)	23.4 ± 8.81	18.2 ± 5.60	1.03 ± 0.9	1.06 ± 0.42	0.618 ± 0.116	0.443 ± 0.175
Oatb1b2(–/–) mice						
C_{max} (ng/mL)	5,610 ± 1,060	4,300 ± 708	5,060 ± 964†,*	1,780 ± 426†	190 ± 46.1	96.4 ± 59.9
AUC_{last} (μg × hour/mL)	18.0 ± 3.87	16.4 ± 7.12	23.9 ± 4.57†,*	7.59 ± 1.39†	0.772 ± 0.084	0.409 ± 0.158

Data represent mean ± SD.
AUC_{last}, area under the plasma concentration–time curve; C_{max}, peak plasma concentration; Oatp, organic anion-transporting polypeptide.
An unpaired *t*-test **P* < 0.05 female vs. male, †*P* < 0.05 Oatp1b2 (–/–) vs. wild-type mice (*n* = 10 per group).

that the estimated metabolic clearance of RG is significantly lower in female mice than in male mice. Plots with estimated regorafenib, regorafenib-N-oxide, and RG concentrations in the presence and absence of Oatp1b2, based on the population pharmacokinetic parameters, in male and female mice are shown in **Figure S4**.

DISCUSSION

Using population-based parent-metabolite modeling, we found in this study that Oatp1b2 and sex strongly impact the systemic exposure to RG in mice receiving oral regorafenib. Metabolic studies revealed that the

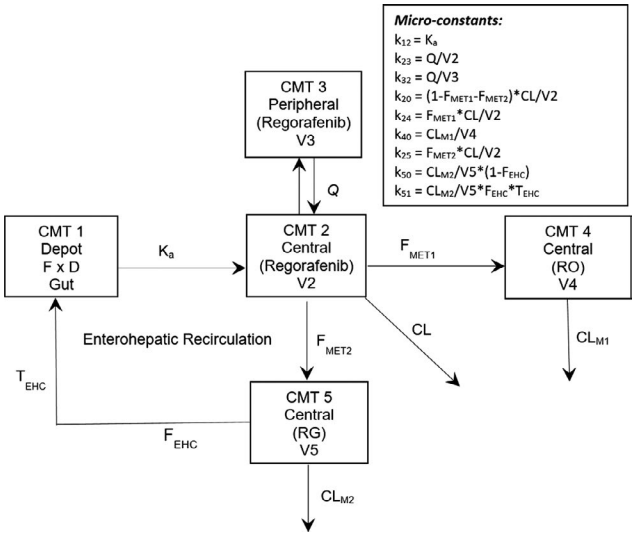

Figure 3 Pharmacokinetic model for regorafenib and its metabolites regorafenib-N-oxide (RO) and regorafenib-glucuronide (RG). CL_{M1}, RO clearance; CL_{M2}, RG clearance; D, regorafenib dose; F, oral bioavailability; K_a, absorption rate constant; Oatp, organic anion-transporting polypeptide; CL, regorafenib clearance; V2, volume of distribution for the central compartment of regorafenib; V3, volume of distribution for the peripheral compartment of regorafenib; V4, volume of distribution for RO; V5, volume of distribution for RG; Q, intercompartmental clearance; F_{MET1}, metabolism of RO; F_{MET2}, metabolism of RG; F_{EHC}, excretion of RG from central compartment to gall bladder; T_{EHC}, reduction rate of RG deconjugation to regorafenib.

liver microsomal expression of Cyp3a11 is twofold lower in female mice, whereas Ugt1a9 levels and function are not sex dependent. This finding is consistent with the metabolism of regorafenib occurring via two competing pathways, and the lack of Oatp1b2 results in decreased clearance of RG.

Recent investigations have demonstrated that regorafenib modestly inhibits the function of human OATP1B1,[16] and that HEK293 cells overexpressing OATP1B1 exhibit increased sensitivity to regorafenib,[17] suggesting that this multikinase inhibitor might be a transported substrate of Oatp1b-type carriers *in vivo*. Our current studies, however, demonstrated that Oatp1b2 deficiency in mice does not cause differences in the pharmacokinetic profile of regorafenib after oral administration. We previously showed that Oatp1b2 (–/–) mice do not have significantly altered expression of metabolic enzymes or transporters in the liver.[18] Furthermore, in these transporter knockout mice, we found that the oxidative metabolism of sorafenib, which is dependent on Cyp3a11, is unchanged.[18,19] These studies were extended here by demonstrating that the baseline expression and function of Ugt1a9, the primary enzyme involved in regorafenib glucuronidation, is also unaffected by Oatp1b2-deficiency. Furthermore, our *in vivo* data are in agreement with studies performed in Eisai hyperbilirubinemic rats suggesting that hepatocellular transport of regorafenib *in vivo* may not be mediated by Oatp1b-type transporters.[20] It should be pointed out that mouse hepatocytes express multiple Oatp1a-type transporters that can potentially provide

Table 3 Population pharmacokinetics of regorafenib, regorafenib-N-oxide, and regorafenib-glucuronide in mice

Parameters	Estimate	%RSE	BE (95% CI)	
CL/F (mL/hour)	0.629	6.33	0.631	0.565–0.734
V2 (mL)	33.8	13.5	34.5	25.0–47.6
V3 (mL)	44.1	13.4	44.0	31.7–57.2
Q/F (mL/hour)	15.1	15.9	14.4	6.20–18.4
CL_{M1} (mL/hour)	1.30	7.32	1.30	1.15–1.53
CL_{M2} (mL/hour)	0.598	21.1	0.607	0.371–0.875
K_a ($hour^{-1}$)	1.08	12.2	1.10	0.761–1.47
F_{EHC}	0.340[a]	–	0.340	0.340
F_{MET1}	0.280[a]	–	0.280	0.280
F_{MET2}	0.170[a]	–	0.170	0.170
T_{EHC}	0.090[a]	–	0.090	0.090
Sex	2.34	26.6	2.44	1.34–3.96
Oatp1b2	5.69	22.8	5.87	3.54–9.51
IIV (variances and %CV)				
IIV-CL/F	0.017 (13.3)	42.7	0.017	0.003–0.032
IIV-V2	0.193 (43.9)	42.3	0.184	0.060–0.359
IIV-V3	0.153 (39.1)	54.4	0.153	0.000–0.390
IIV-CL_{M2}	0.198 (44.5)	34.5	0.188	0.068–0.324
IIV-K_a	0.143 (37.8)	42.4	0.156	0.038–0.307
RV (%CV)				
Regorafenib	3.34	14.6	3.37	2.48–4.41
RG	27.0	15.7	27.1	19.5–34.9
RO	7.38	20.1	7.35	4.92–10.6

%CV, coefficient of variation; BE, backward elimination; CI, confidence interval; CL/F, total clearance; CL_{M1}, regorafenib-N-oxide clearance; CL_{M2}, regorafenib-glucuronide clearance; FEHC, excretion of RG from central compartment to gall bladder; F_{MET1}, metabolism of RO; F_{MET2}, metabolism of RG; IIV, interindividual variability; K_a, absorption rate constant; Oatp, organic anion-transporting polypeptide; Q/F, intercompartmental clearance; RG, regorafenib-glucuronide; RO, regorafenib-N-oxide; RV, residual variability. RSE, residual standard error; TEHC, reduction rate of RG deconjugation to regorafenib; V2, volume of distribution for the central compartment of regorafenib; V3, volume of distribution for the peripheral compartment of regorafenib

[a]F_{MET1}, F_{MET2}, F_{EHC}, and T_{EHC} were fixed based on the literature value.[9]

compensatory restoration of function when Oatp1b2 activity is lost,[21] and this could have potentially confounded the current study results. This potential limitation of the Oatp1b2 (–/–) mouse model, however, was not substantiated in a prior study indicating that the pharmacokinetic profile of sorafenib was essentially the same in Oatp1b2 (–/–) mice when compared with that observed in mice that are deficient in Oatp1a-members as well as Oatp1b2 (Oatp1a/1b (–/–) mice).[10] Although not experimentally verified, it is reasonable to speculate that possible compensatory effects of Oatp1a-type transporters did not influence the results of our current studies with regorafenib. Based on these collective findings suggesting an apparent lack of interaction of sorafenib and regorafenib with Oatp1a-type or Oatp1b-type transporters *in vivo*, it is likely that additional, currently unidentified uptake transporters of these agents exist that contribute to the hepatic elimination profiles in mice.

In contrast to regorafenib or its pharmacologically active metabolite regorafenib-N-oxide,[22] the AUC_{last} of RG was

significantly increased in Oatp1b2 (–/–) compared with wild-type mice. No significant difference in the rate of isolated RG formation was observed between liver microsomes from mice with or without Oatp1b2, indicating that the observed kinetic process differences were due to abnormalities in transport. A similar phenomenon was previously reported for sorafenib in which Oatp1b2 (–/–) mice showed excessive accumulation of sorafenib-glucuronide in the systemic circulation due to a defective mechanism called "hepatocyte hopping."[21] Under normal physiological conditions, this same hepatocyte hopping principle is likely to be operational for RG, in order to facilitate the excretion of phase II-coupled metabolites into the bile to avoid hepatic accumulation of potentially toxic substances.

The potential clinical ramification of the hepatocyte-hopping phenomenon of RG requires additional investigation. Regorafenib was recently demonstrated to undergo intestinal recirculation,[23] in a manner that may be dependent on bacterial β-glucuronidase-mediated deconjugation of RG within the intestinal lumen.[24] Based on these prior insights, it can be surmised that inhibition of Oatp1b2-mediated transport of RG can diminish hepatocellular accumulation and impaired biliary excretion, and lead to diminished enterohepatic recycling and subsequently result in reduced plasma levels of regorafenib following repeat administration cycles. This interference with intestinal hepatic recirculation has been previously reported with the immunosuppressive drug mycophenolate mofetil, which undergoes extensive glucuronidation in the liver.[25] In this context, it is noteworthy to point out that intentional interference of the intestinal deconjugation of RG as well as the glucuronide acid conjugate of regorafenib-N-oxide by repeat administration of the nonabsorbable antibiotic neomycin decreases the systemic exposure to regorafenib-N-oxide by 76% without affecting the mean AUC of regorafenib itself.[9] Additional studies are required to evaluate the effects of other antibiotics on measures of systemic exposure to regorafenib in order to confirm a role of RG in its enterohepatic recirculation.

In conclusion, a population pharmacokinetic model was developed for regorafenib in mice that provides a tool to quantitatively predict the transporter-mediated absorption and disposition patterns of regorafenib and its two main metabolites regorafenib-N-oxide and RG. A potential limitation of the model resides in the fact that some parameters represent fixed values based on human data, suggesting that further refinements may be possible in the future. Nonetheless, the developed parent-metabolite model suggests that Oatp1b2 and sex strongly influence the exposure to RG in mice receiving oral regorafenib, and that Oatp1b2 and sex were two significant covariates on the metabolic clearance of this metabolite. The model provides mechanistic insights into the *in vivo* disposition of regorafenib and can be applied to study the potential for transporter-mediated drug interactions with other xenobiotics undergoing extensive glucuronidation.

Supporting Information. Supplementary information accompanies this paper on the *Clinical and Translational Science* website (www.cts-journal.com).

Figure S1. Goodness-of-fit plots for the final pharmacokinetic model of regorafenib (circles), regorafenib-glucuronide (squares), and regorafenib-N-oxide (triangles) in mice.
Figure S2. Visual predictive check of the final model for regorafenib (**a**), regorafenib-glucuronide (**b**), and regorafenib-N-oxide (**c**) observations in mice.
Figure S3. Model differential equations.
Figure S4. Time courses of observed data (mean ± SD) and model-predicted (PRED) plasma concentrations of regorafenib (**a**), regorafenib-N-oxide (**b**), and regorafenib-glucuronide (**c**) following a 10 mg/kg oral dose of regorafenib in Oatp1b2 (–/–) and wild-type mice.

Acknowledgments. We would like to thank Richard Kim and Jeffrey Stock for providing the Oatp1b2 (–/–) mice.

Funding. The project was supported in part by National Institutes of Health (NIH) grant R01 CA138744 (S.D.B.) and by the OSU Comprehensive Cancer Center using Pelotonia funds. The content is solely the responsibility of the authors and does not necessarily represent the official views of the funding agencies.

Conflict of Interest. The authors declared no competing interests for this work.

Author Contributions. Q.F., A.S., and S.D.B. wrote the manuscript. Q.F., A.S., and S.D.B. designed the research. Q.F., M.C., J.T.A., X.S., and S.H. performed the research. Q.F., M.C., A.S., and S.D.B. analyzed the data.

1. Dhillon, S. Regorafenib: a review in metastatic colorectal cancer. *Drugs* **78**, 1133–1144 (2018).
2. Agulnik, M. & Attia, S. Growing role of regorafenib in the treatment of patients with sarcoma. *Target Oncol.* **13**, 417–422 (2018).
3. Heo, Y.A. & Syed, Y.Y. Regorafenib: a review in hepatocellular carcinoma. *Drugs* **78**, 951–958 (2018).
4. Tlemsani, C. *et al.* Effect of glucuronidation on transport and tissue accumulation of tyrosine kinase inhibitors: consequences for the clinical management of sorafenib and regorafenib. *Expert Opin. Drug Metab. Toxicol.* **11**, 785–794 (2015).
5. Longue, M. *et al.* The importance of jointly analyzing treatment administration and toxicity associated with targeted therapies: a case study of regorafenib in soft tissue sarcoma patients. *Ann. Oncol.* **29**, 1588–1593 (2018).
6. Edginton, A.N., Zimmerman, E.I., Vasilyeva, A., Baker, S.D. & Panetta, J.C. Sorafenib metabolism, transport, and enterohepatic recycling: physiologically based modeling and simulation in mice. *Cancer Chemother. Pharmacol.* **77**, 1039–1052 (2016).
7. Wang, Y.K., Xiao, X.R., Xu, K.P. & Li, F. Metabolic profiling of the anti-tumor drug regorafenib in mice. *J. Pharm. Biomed. Anal.* **159**, 524–535 (2018).
8. Fu, Q. *et al.* Development and validation of an analytical method for regorafenib and its metabolites in mouse plasma. *J. Chromatogr. B Analyt. Technol. Biomed. Life Sci.* **1090**, 43–51 (2018).
9. Gerisch, M. *et al.* Mass balance, metabolic disposition, and pharmacokinetics of a single oral dose of regorafenib in healthy human subjects. *Cancer Chemother. Pharmacol.* **81**, 195–206 (2018).
10. Zimmerman, E.I. *et al.* Contribution of OATP1B1 and OATP1B3 to the disposition of sorafenib and sorafenib-glucuronide. *Clin. Cancer Res.* **19**, 1458–1466 (2013).
11. Choi, Y.H. & Yu, A.M. ABC transporters in multidrug resistance and pharmacokinetics, and strategies for drug development. *Curr. Pharm. Des.* **20**, 793–807 (2014).
12. Huh, Y., Hynes, S.M., Smith, D.E. & Feng, M.R. Importance of peptide transporter 2 on the cerebrospinal fluid efflux kinetics of glycylsarcosine characterized by nonlinear mixed effects modeling. *Pharm. Res.* **30**, 1423–1434 (2013).
13. Hurtado, F.K., Weber, B., Derendorf, H., Hochhaus, G. & Dalla Costa, T. Population pharmacokinetic modeling of the unbound levofloxacin concentrations in rat plasma and prostate tissue measured by microdialysis. *Antimicrob. Agents Chemother.* **58**, 678–686 (2014).
14. Brochot, A., Zamacona, M. & Stockis, A. Physiologically based pharmacokinetic/pharmacodynamic animal-to-man prediction of therapeutic dose in a model of epilepsy. *Basic Clin. Pharmacol. Toxicol.* **106**, 256–262 (2010).
15. Shord, S.S. Regorafenib (Stivarga®). Pharmacology/toxicology nda review and evaluation. FDA. 2012.4.30 <https://www.accessdata.fda.gov/drugsatfda_docs/nda/2012/203085Orig1s000PharmR.pdf>.

16. Leblanc, A.F. *et al.* OATP1B2 deficiency protects against paclitaxel-induced neurotoxicity. *J. Clin. Invest.* **128**, 816–825 (2018).
17. Ohya, H., Shibayama, Y., Ogura, J., Narumi, K., Kobayashi, M. & Iseki, K. Regorafenib is transported by the organic anion transporter 1B1 and the multidrug resistance protein 2. *Biol. Pharm. Bull.* **38**, 582–586 (2015).
18. Lancaster, C.S. *et al.* OATP1B1 polymorphism as a determinant of erythromycin disposition. *Clin. Pharmacol. Ther.* **92**, 642–650 (2012).
19. Vasilyeva, A. *et al.* Hepatocellular shuttling and recirculation of sorafenib-glucuronide is dependent on Abcc2, Abcc3, and Oatp1a/1b. *Cancer Res.* **75**, 2729–2736 (2015).
20. Hotta, K. *et al.* Lack of contribution of multidrug resistance-associated protein and organic anion-transporting polypeptide to pharmacokinetics of regorafenib, a novel multi-kinase inhibitor, in rats. *Anticancer Res.* **35**, 4681–4689 (2015).
21. Iusuf, D., van de Steeg, E. & Schinkel, A.H. Functions of OATP1A and 1B transporters in vivo: insights from mouse models. *Trends Pharmacol. Sci.* **33**, 100–108 (2012).
22. van de Steeg, E. *et al.* Complete OATP1B1 and OATP1B3 deficiency causes human Rotor syndrome by interrupting conjugated bilirubin reuptake into the liver. *J. Clin. Invest.* **122**, 519–28 (2012).
23. Zopf, D. *et al.* Pharmacologic activity and pharmacokinetics of metabolites of regorafenib in preclinical models. *Cancer Med.* **5**, 3176–3185 (2016).
24. Hilger, R.A. *et al.* Pharmacokinetics of sorafenib in patients with renal impairment undergoing hemodialysis. *Int. J. Clin. Pharmacol. Ther.* **47**, 61–64 (2009).
25. Picard, N. *et al.* The role of organic anion-transporting polypeptides and their common genetic variants in mycophenolic acid pharmacokinetics. *Clin. Pharmacol. Ther.* **87**, 100–108 (2010).